Research Article | Vol. 24, No. 17 | 22 Aug 2016 | OPTICS EXPRESS 19195

Optics EXPRESS

Moisture-insensitive optical fingerprint scanner based on polarization resolved in-finger scattered light

SEON-WOO BACK,[1] YONG-GEON LEE,[1] SANG-SHIN LEE,[1,*] AND GEUN-SIK SON[2]

[1]*Department of Electronic Engineering, Kwangwoon University, 20 Kwangwoon-ro, Nowon-gu, Seoul 01897, South Korea*
[2]*Fire Insurers Laboratories of Korea (FLIK), Yeoju 12661, South Korea*
**slee@kw.ac.kr*

Abstract: A moisture-insensitive optical fingerprint scanner (FPS) that is based on polarization resolved in-finger light is proposed and realized. Incident visible light, which is selectively fed to a fingerprint sample via a polarization beam splitter (PBS), is deemed to be partially scattered backward by tissues associated with the skin of the finger. The backscattered light is mostly index-guided in the ridge comprising the fingerprint, which has a higher refractive index, and is drastically dispersed in the valley, which is typically filled with water or air and so has a lower index. However, when light reflects directly off the surface of the finger skin, it fundamentally prevents the scanned image from being determined. The proposed FPS produces bright and dark intensity patterns that are alternately created on the surface of the PBS and correspond to the ridges and valleys, respectively. Thus, this method can especially distinguish between a fake synthetic fingerprint and a genuine fingerprint due to its use of in-finger scattered light. The scanner has been rigorously designed by carrying out ray-optic simulations depending on the wavelength, with tissue-induced scattering taken into account. The device was constructed by incorporating a wire-grid type PBS in conjunction with visible LED sources, including blue, green and red. The scanner adopting a blue LED, which exhibits the strongest light scattering, resulted in the best fingerprint image, enabling enhanced fidelity under the wet and dry situations. Finally, a fake synthetic fingerprint could be successfully discriminated.

OCIS codes: (230.0230) Optical devices; (290.0290) Scattering; (110.0110) Imaging systems; (170.0170) Medical optics and biotechnology

References and links

1. X. Xia and L. O. Gorman, "Innovations in fingerprint capture devices," Pattern Recognit. **36**(2), 361–369 (2003).
2. M. S. Alam and M. A. Karim, "Biometric recognition systems: introduction," Appl. Opt. **44**(5), 635–636 (2005).
3. D. Maltoni, D. Maio, A. K. Jain, and S. Prabhakar, *Handbook of Fingerprint* (Springer, 2009), Chap. 2.
4. Y. Jie and Z. Jihong, "Fingerprint sensor using a polymer dispersed liquid crystal holographic lens," Appl. Opt. **49**(25), 4763–4766 (2010).
5. R. K. Rowe, K. A. Nixon, and P. W. Butler, "Multispectral fingerprint image acquisition," in *Advances in Biometrics*, N. K. Ratha and V. Govindaraju, ed. (Springer, 2008).
6. S. Memon, M. Sepasian, and W. Balachandran, "Review of fingerprint sensing technologies," in *Proceedings of 12th IEEE International Multitopic Conference* (IEEE, 2008), pp. 226–231.
7. S. Memon, N. Manivannan, A. Noor, W. Balachadran, and N. V. Boulgouris, "Fingerprint sensors:liveness detection issue and hardware based solutions," Sensors Transducers J. **136**(1), 35–49 (2012).
8. V. Tuchin, "Light scattering study of tissues," Phys.- Usp **40**(5), 495–515 (1997).
9. R. R. Anderson and J. A. Parrish, "The optics of human skin," J. Invest. Dermatol. **77**(1), 13–19 (1981).
10. T. Lister, P. A. Wright, and P. H. Chappell, "Optical properties of human skin," J. Biomed. Opt. **17**(9), 090901 (2012).
11. J. D. van der Laan, J. B. Wright, D. A. Scrymgeour, S. A. Kemme, and E. L. Dereniak, "Evolution of circular and linear polarization in scattering environments," Opt. Express **23**(25), 31874–31888 (2015).
12. I. A. Vitkin and R. C. N. Studinski, "Polarization preservation in diffusive scattering from in vivo turbid biological media: effects of tissue optical absorption in the exact backscattering direction," Opt. Commun. **190**(1-6), 37–43 (2001).

#268761 http://dx.doi.org/10.1364/OE.24.019195
Journal © 2016 Received 20 Jun 2016; revised 1 Aug 2016; accepted 1 Aug 2016; published 10 Aug 2016

Optics EXPRESS

13. M. C. Pierce, J. Strasswimmer, B. Hyle Park, B. Cense, and J. F. De Boer, "Birefringence measurements in human skin using polarization-sensitive optical coherence tomography," J. Biomed. Opt. **9**(2), 287–291 (2004).
14. S. Morgan and M. Ridgway, "Polarization properties of light backscattered from a two layer scattering medium," Opt. Express **7**(12), 395–402 (2000).
15. V. Tuchin and V. V. Tuchin, *Tissue Optics: Light Scattering Methods and Instruments for Medical Diagnosis*, (SPIE, 2007) Chap. 1.
16. J. Mobley, T. V. Dinh, and V. V. Tuchin, "Optical properties of tissue," in *Biomedical Photonics Handbook: Fundamentals, Devices, and Techniques*, T. V. Dinh, ed. (CRC Press, 2014).
17. A. Bhandari, B. Hamre, Ø. Frette, K. Stamnes, and J. J. Stamnes, "Modeling optical properties of human skin using Mie theory for particles with different size distributions and refractive indices," Opt. Express **19**(15), 14549–14567 (2011).
18. D. Maltoni, D. Maio, A. K. Jain, and S. Prabhakar, *Handbook of Fingerprint Recognition* (Springer, 2009) Chaps. 1 and 3.
19. J. S. Han, Z. Y. Tan, K. Sato, and M. Shikida, "Thermal characterization of micro heater arrays on a polyimide film substrate for fingerprint sensing applications," J. Micromech. Microeng. **15**(2), 282–289 (2005).
20. T. Matsumoto, H. Masumoto, K. Yamada, and S. Hoshino, "Impact of artificial "gummy" fingers on fingerprint systems," Proc. SPIE **4677**, 275–289 (2002).

1. Introduction

A variety of biometric recognition systems based on the fingerprint, iris, vein or face have been extensively developed as alternatives for conventional token-based authentification systems that mostly rely on an identification card and password [1,2]. Fingerprint identification is of particular concern due to its uniqueness, permanence, and collectability, which can be largely classified into optical types (including techniques that use the frustrated total internal reflection (FTIR), hologram, multi-spectral imaging and in-finger light dispersion) and non-optical types (which takes advantage of the capacitance, radio frequency, acoustic wave, and thermal detection) [3–6]. Optical recognition has perceived advantages in that it is impervious to ubiquitous electro-magnetic interference and electrostatic discharge. However, the most prevalent FTIR-based fingerprint recognition methods are fatally incapable of distinguishing synthetic fingerprints from genuine human fingerprints. In addition, its performance is seriously degraded in wet conditions [7]. In this paper, we propose and build a moisture-proof FPS that solely takes advantage of in-finger scattered light in order to mitigate issues with previous approaches. A polarizing beam splitter (PBS) cube is introduced to selectively route incident light into the fingerprint sample, thereby inducing light to backscatter within the finger skin. Thus, light is highly confined in ridges with a higher refractive index and is severely dispersed in valleys with a lower index. Bright and dark intensity patterns manifest on the surface of the PBS in correspondence with the ridge and valley, respectively. The proposed scanner is notable in that it differentiates a fake synthetic fingerprint from an authentic one, due to its unique reliance on the in-finger scattered light instead of externally reflected light. This scanner was meticulously designed and evaluated via wavelength-based ray-optic simulations, with tissue-induced scattering taken into account. The device was then constructed by employing a wire-grid type PBS in conjunction with visible LED sources of different colors. The scanner incorporating a blue source provided the best fingerprint image, enabling improved fidelity under both wet and dry situations while also distinctly discriminating a fake synthetic fingerprint.

2. Proposed FPS exploiting polarization-resolved in-finger light and its design

The proposed FPS incorporates polarization-resolved in-finger scattered light, and it is comprised of a PBS cube, a visible LED source, a collimating lens, and an imaging CCD camera. A beam emanating from the source is collimated to enter into the PBS cube, decomposing into two orthogonal components with perpendicular polarization (s-pol) and parallel polarization (p-pol) according to their E-field alignment, as shown in Fig. 1(a). The incoming s-pol light is routed toward the finger under test, which is gently placed on top of the cube, while incident p-pol light proceeds straight through the cube. The s-pol light impinging upon the finger is supposed to partially undergo a Fresnel reflection at the PBS-

Optics EXPRESS

finger interface, so as to penetrate into the finger. Penetrated light is known to substantially scatter in tissues associated with the finger skin [8]. The in-finger light, alluding to the scattered light which propagates backward in the direction of the PBS cube, delivers both p-pol and s-pol components as a result of scattering induced variations in polarization. As depicted in Fig. 1(b), only the p-pol in-finger component is transmitted through the PBS to reach the CCD camera, whereas the s-pol component deflects sideways. It is important to mention that the external s-pol light reflecting directly off the surface of the finger is fundamentally prohibited from reaching the imaging camera through the mediation of the PBS.

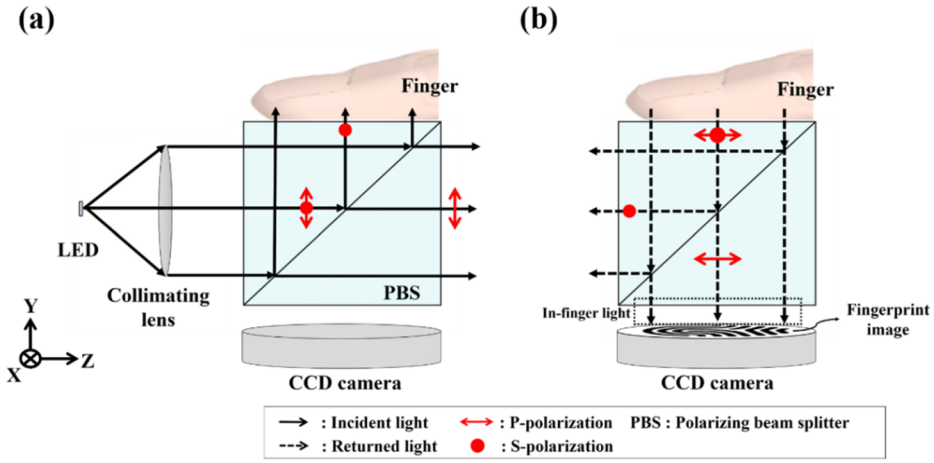

Fig. 1. Configuration of the proposed FPS and its beam trajectory depending on the polarization for (a) the incident light and (b) the backscattered in-finger light in addition to the light directly originating from the finger surface via the Fresnel reflection.

The feasibility of the proposed FPS is assessed by elaborating on the generation of polarization-resolved backscattered in-finger light by approximately modelling the structure of the finger skin. The fingerprint is usually engraved in a layer of epidermis that forms on top of the dermis layer of human skin. As described in Fig. 2(a), the incident s-pol light is partially Fresnel-reflected at the air-skin boundary by an amount ranging from 4 to 7% [9,10]. The rest of the light enters into the epidermis to subsequently experience multiple scattering within the mesh of tissues. Considering that the state of polarization is categorically subjected to the scattering process, part of the incident s-pol component is converted into a p-pol component [11–14]. Hence, the scattered light propagating in the backward direction, which is of principal interest from the standpoint of our FPS, is presumed to exhibit both the s- and p-pol states of polarization. However, the s-pol component is blocked and only the p-pol scattered component will pass through the PBS to ultimately arrive at the CCD camera. As depicted in Fig. 2(a), the fingerprint is comprised of a group of grooves and is assumed to be placed right on top of the PBS cube. The fingerprint pattern has a depth of D and may be emulated by ridges and valleys that are respectively made up of epidermis and air. The epidermis has much larger refractive index (n = ~1.5) than air [8].

The transmission of in-finger scattered light through the fingerprint is shown in greater detail in Fig. 2(b). In the ridge, the scattered light is preferentially index guided towards the surface of the finger by virtue of the sufficient index contrast between the epidermis and air, although there still exists a small amount of backscattered light. To the contrary, in-finger light travelling in the valley tends to be significantly refracted and scattered at the boundary between the epidermis and air, being subsequently dispersed in air so as to shine the top surface of the PBS cube. Hence, the ridges and valleys in the fingerprint are translated into

Optics EXPRESS

bright and dark patterns that form on top of the PBS cube, respectively. The observed pattern is anticipated to become even more distinct as the wavelength is shortened to reinforce the scattering [15]. In the case of the valleys, the in-finger light is additionally attenuated as a result of successive Fresnel reflections both at the air-PBS and air-epidermis boundaries, unlike in the case of the ridge. As a consequence, a standout intensity contrast is attained between the valley and the ridge regions at the site on the top surface of the PBS, mimicking the original fingerprint pattern.

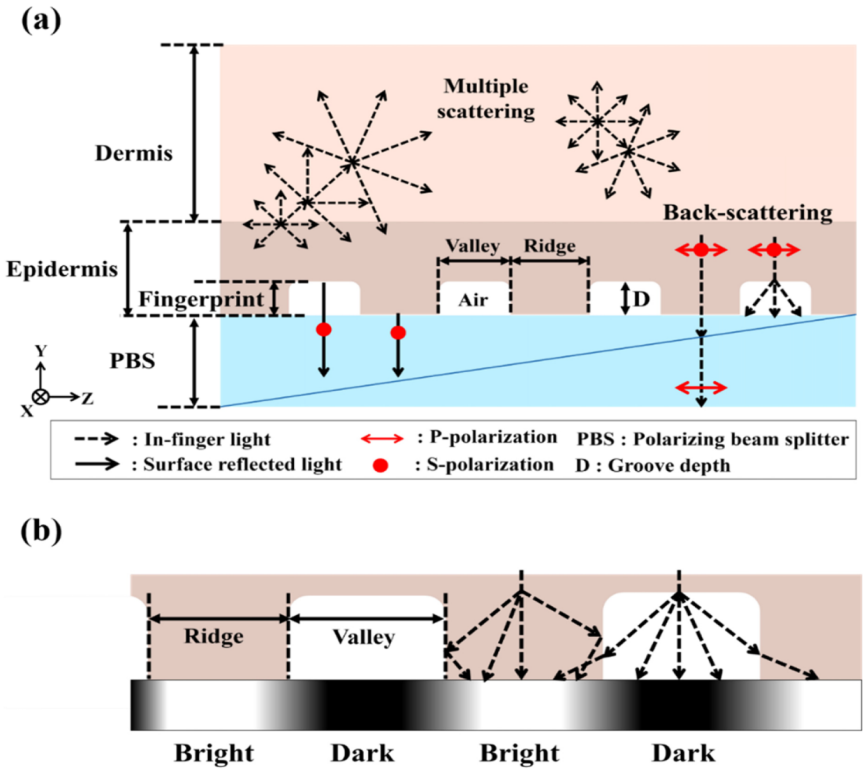

Fig. 2. (a) Modeling of a fingerprint, with the trajectory of various optical rays described. (b) Process of transferring the ridge and valley to a bright and dark region, respectively.

We thoroughly examined the operation of the proposed FPS through ray-optic simulations assisted by LightTools, a tool that adequately handles the light scattering incurred by the tissues constituting the finger skin [16,17]. Figure 3(a) shows a cross-section of the modelled structure together with its bottom view. A typical human fingerprint pattern has a period of around 500 μm, with a width of the ridge ranging from 100 to 300 μm, so the structural parameters were determined to exhibit a ridge width of 100 μm, a period of 200 μm, and a groove depth of 50 μm [18,19]. To emulate the in-finger light, a visible light source operating at $\lambda = 488$ nm was positioned to illuminate the light on the fingerprint. It should be noted that the receiver is supposed to exhibit an angle of acceptance of $\theta = 8°$ considering the angular limitations associated with a PBS that will be used for the experiment. The performance of our FPS was then concretely validated by specifically taking into account both dry and wet situations. Figure 3(b) reveals the fingerprint image that was calculated and its intensity profile along the Z-axis under the dry condition. An intensity contrast, which is defined as the ratio of the maximum intensity of the ridge to the minimum intensity of the valley, is vividly

Optics EXPRESS

observed between the valley and the ridge in a periodic manner, with the ridge providing higher intensity levels than the valley, as predicted. The obtained fingerprint presents a pitch of ~100 μm. The results regarding the wet condition are given in Fig. 3(c), where an equivalent level of periodic intensity contrast is observed in the calculated image. The calculated intensity contrast is nearly 2.0 for the dry condition while it declines to ~1.1 for the wet condition. Although the calculated contrast for the wet condition is seriously reduced compared to the dry condition, as shown in Figs. 3(b) and 3(c), it has been confirmed a reliable recognition can be practically achieved by treating the obtained fingerprint image with the help of image processing techniques such as a local adaptive thresholding in conjunction with a smoothing.

The proposed FPS exploits polarization-resolved in-finger light and efficiently discriminates between a fake and an authentic fingerprint. An FTIR type FPS resorts to an index contrast between the ridge and valley and inevitably malfunctions with a fake fingerprint, made of synthetic polymer materials, whose refractive indices in the proximity of that of human skin (such as latex, silicone, gelatin and PDMS) [18,20]. When a synthetic sample is applied to the proposed FPS, where the in-finger scattered light plays the role of chiefly producing fingerprint pattern, light reflecting off the surface of fake skin is inherently inhibited from accessing the PBS. Moreover, no scattering can be induced due to the absence of skin tissue as scatterer, and therefore our FPS is predicted to obtain no meaningful pattern in response to a synthetic fingerprint.

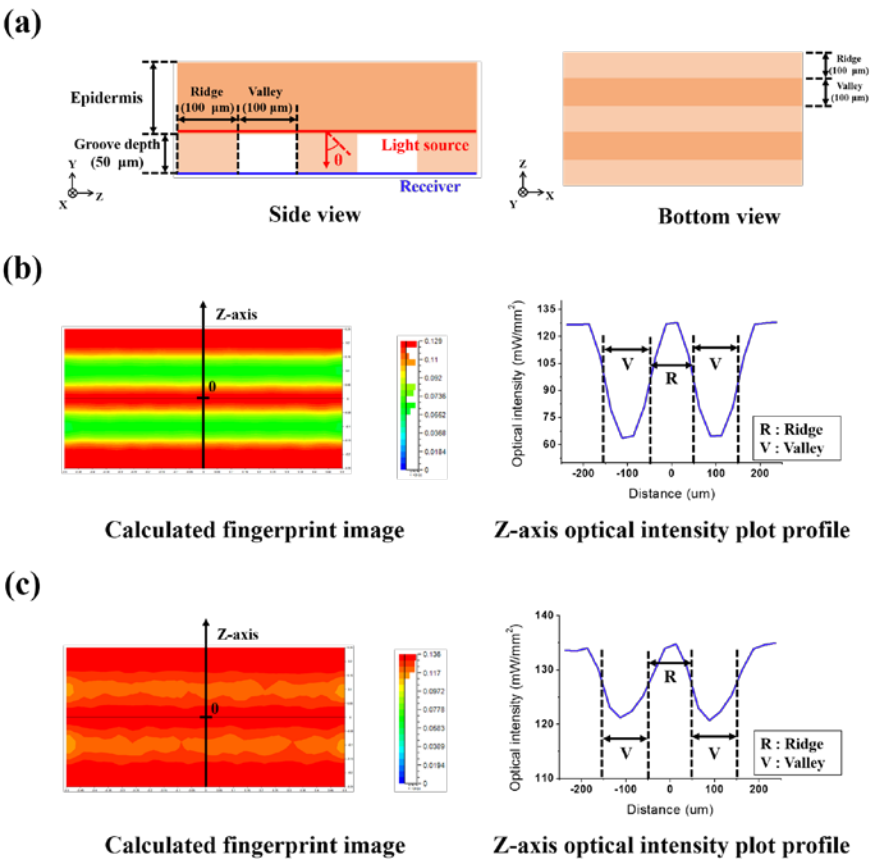

Fig. 3. (a) Structure of a modelled fingerprint pattern. (b) Calculated fingerprint image under the dry condition and its intensity profile. (c) Calculated fingerprint image under the wet condition and its intensity profile.

Optics EXPRESS

3. Embodiment of the proposed FPS and its characterization

As displayed in Fig. 4(a), the proposed FPS was constructed utilizing a wire-grid type PBS cube (WPBS254-VIS, Thorlabs, USA), in conjunction with three visible LED light sources of blue, green, and red color corresponding to λ = 455 nm, 530 nm and 625 nm, respectively. A CCD camera with an objective lens (378-802-6, Mitutoyo, Japan) captured the light stemming from the scanner, specifically imaging the boundary between the fingerprint and the PBS cube. Figure 4(b) shows a photograph of an actual fingerprint sample taken by the camera during the test. The structural parameters were monitored under no excessive pressure, and the ridge and valley are about 190 μm and 140 μm wide, respectively, exhibiting a pitch of 330 μm. The fingerprint sample was also inspected with a commercial FTIR-based device.

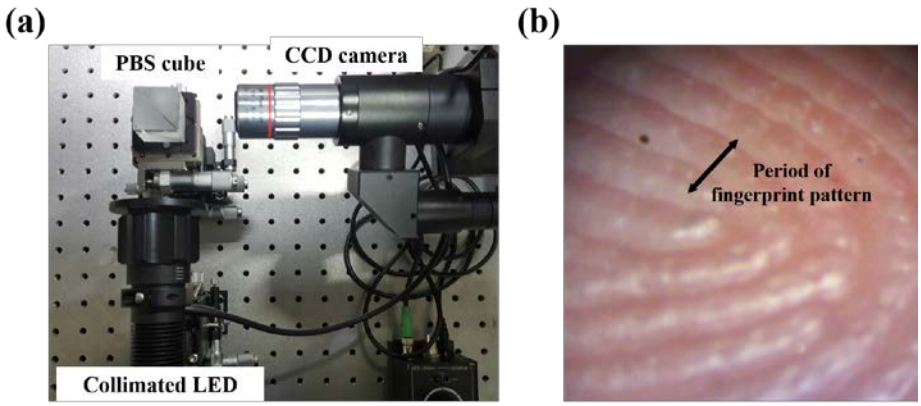

Fig. 4. (a) Completed FPS incorporating a wire-grid type PBS in combination with visible collimated LEDs. (b) Photograph of an actual fingerprint sample of concern.

We used the prepared FPS in the dry condition to individually acquire a fingerprint image relevant to the aforementioned sample with three different light sources, as shown in Fig. 5(a). The measured fingerprint images were slightly processed in terms of the intensity contrast. The image obtained with the blue source, which had the shortest wavelength, showed clearly distinct ridges and valleys. A light intensity profile is also plotted along the arrow in white, exhibiting a substantial contrast between the ridge and valley that were approximately 220 and 180 μm wide on average, respectively. Although the image obtained with the green source showed a similar pattern, the contrast in the ridge-valley intensity appears to be slightly less than that obtained with the blue LED. The red source had the longest wavelength, and the fingerprint image was barely discernable, resulting in an unsatisfactory contrast. The quality of the fingerprint images improves as the wavelength decreases for the three LED sources, as anticipated, because the multiple scattering, which is accountable for the generation of backscattered in-finger light, is reinforced for shorter wavelengths. For instance, we may further enhance the quality of the fingerprint image by capitalizing on a UV LED source with shorter wavelengths of around 400 nm compared with the blue light, as long as the UV light is never harmful to the human body.

Under wet conditions, the target fingerprint is initially immersed in water to place a sufficient amount of moisture on the surface thereof, and the corresponding measurements are presented in Fig. 5(b). An adequate fingerprint image could be obtained with blue and green LED sources, giving rise to discernable ridges and valleys. As in the case of the dry condition, the performance of the proposed FPS deteriorates with a longer wavelength. As a result, the moisture-insensitive operation of the proposed FPS has been successfully validated in the experiment. For the manufactured FPS incorporating a blue LED source, the measured intensity contrast was approximately 1.3 for the dry condition and ~1.2 for the wet condition. Although the optical properties of the fingerprint could not be fully taken into account for the

Optics EXPRESS

simulations, reasonable correlations between simulation and measurement results were observed.

Figure 6(a) shows a commercial FTIR-based FPS (Model P1562, Hanjin Data, S. Korea) device that was tested separately to conduct a comparison of the clear fingerprint image obtained under dry conditions and post-processed in binary code. Figure 6(b) then shows how the wet condition resulted in the fingerprint image presenting no useful information enabling a fingerprint recognition, indicating that the TIR has been deactivated because of the notably diminished index contrast between the ridge and valley filled with water. In contrast, the proposed in-finger type FPS functions properly in spite of the presence of moisture, purveying an adequate fingerprint image that might translate into a useful binary pattern through proper signal processing.

We finally performed an experiment to differentiate between an authentic fingerprint and a fake fingerprint made of polydimethylsiloxane (PDMS), as shown in Fig. 7(a). The commercial FTIR type FPS readily replicated the image obtained from the fake fingerprint, as shown in Fig. 7(b). On the other hand, as shown in Fig. 7(c), the proposed FPS rarely responds to the fake fingerprint since it is based on the use of internally scattered light. It is finally speculated the proposed in-finger type scanner can effectively discriminate between an authentic and a fake fingerprint, as desired.

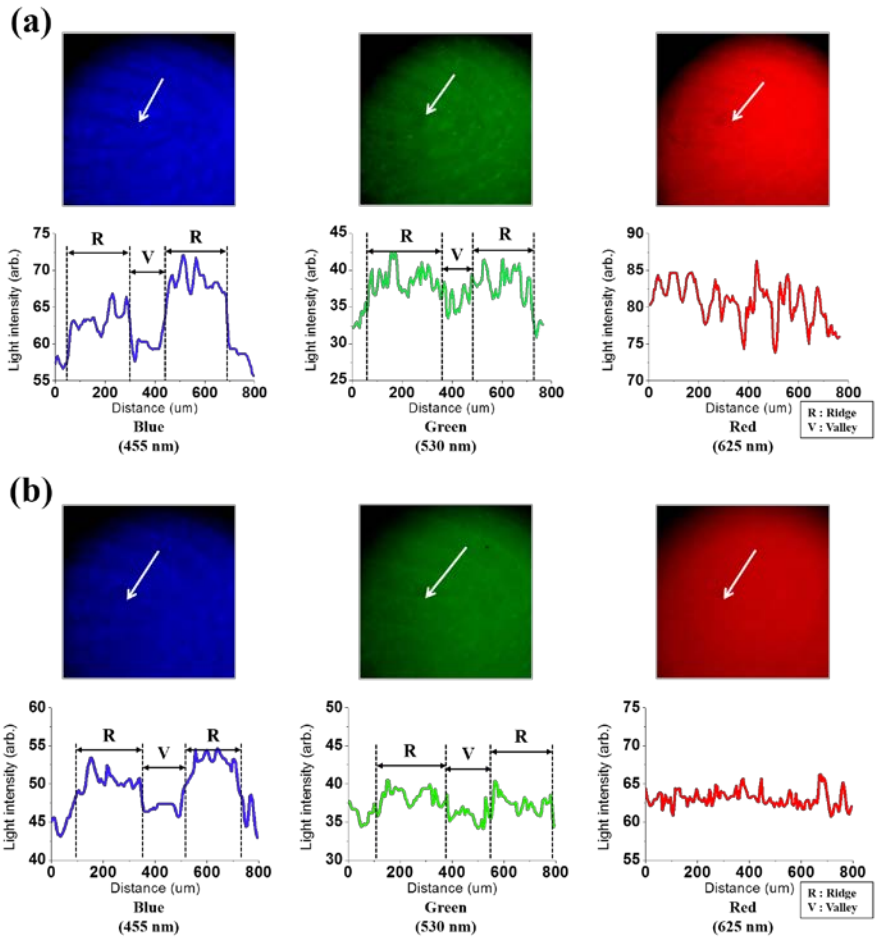

Fig. 5. Measured fingerprint images for various LEDs of blue, green and red and their intensity profiles under (a) dry condition and (b) wet condition.

Optics EXPRESS

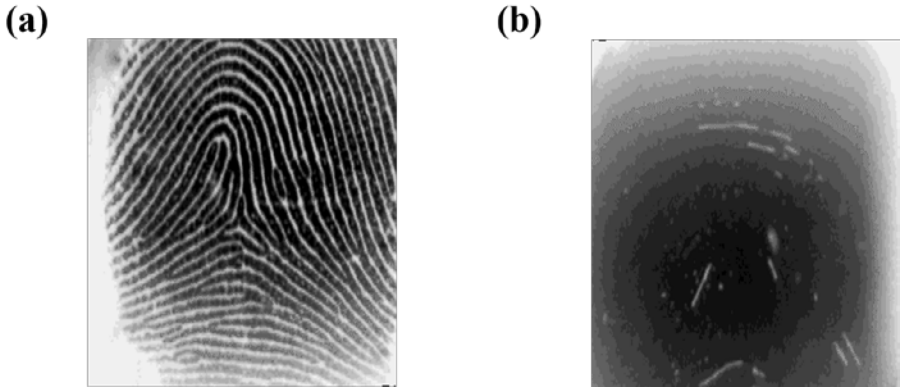

Fig. 6. Acquired fingerprint image for a commercially available FTIR based FPS under (a) dry condition and (b) wet condition.

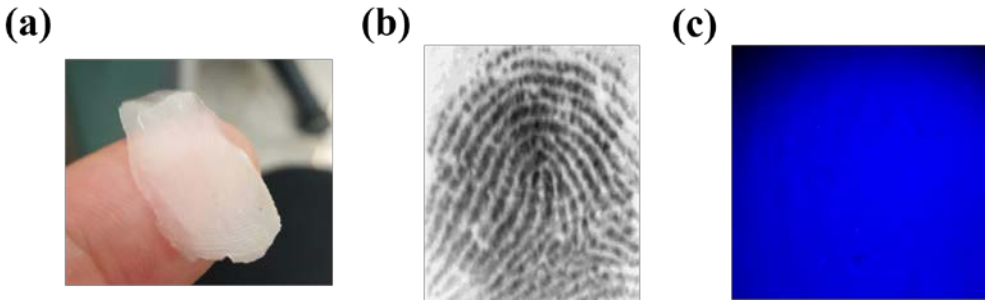

Fig. 7. (a) Prepared synthetic fingerprint in PDMS. Fingerprint images acquired by applying (b) the FTIR based FPS and (c) the proposed FPS.

4. Conclusion

A moisture-proof FPS based on polarization-resolved in-finger scattered light was presented, capable of identifying a fake synthetic fingerprint. By dint of a wire-grid type PBS cube, the backscattered light which originates from inside the finger skin is selectively exploited to create the output fingerprint image, while the light which is directly reflected from the surface of the finger is prohibited. The best quality of fingerprint image, enabling high fidelity to the original fingerprint, was derived from the scanner tapping into a blue LED, which leads to the strongest scattering.

Funding

National Research Foundation of Korea (MSIP) (No. 2016R1A2B2010170); Kwangwoon University.

Acknowledgments

The authors are grateful to Mr. Chanwoo J. Lee, Seoul Foreign School, Seoul, S. Korea, for his help with the preparation of the manuscript.